

# A Highly Selective Copper–Indium Bimetallic Electrocatalyst for the Electrochemical Reduction of Aqueous CO<sub>2</sub> to CO\*\*

Shahid Rasul, Dalaver H. Anjum, Abdesslem Jedidi, Yury Minenkov, Luigi Cavallo, and Kazuhiro Takanabe\*

**Abstract:** The challenge in the electrochemical reduction of aqueous carbon dioxide is in designing a highly selective, energy-efficient, and non-precious-metal electrocatalyst that minimizes the competitive reduction of proton to form hydrogen during aqueous CO<sub>2</sub> conversion. A non-noble metal electrocatalyst based on a copper-indium (Cu–In) alloy that selectively converts CO<sub>2</sub> to CO with a low overpotential is reported. The electrochemical deposition of In on rough Cu surfaces led to Cu–In alloy surfaces. DFT calculations showed that the In preferentially located on the edge sites rather than on the corner or flat sites and that the d-electron nature of Cu remained almost intact, but adsorption properties of neighboring Cu was perturbed by the presence of In. This preparation of non-noble metal alloy electrodes for the reduction of CO<sub>2</sub> provides guidelines for further improving electrocatalysis.

The development of an artificial photosynthesis process that converts CO<sub>2</sub> and stores the energy in the form of chemical bonds is one of the grand challenges in modern chemistry.<sup>[1,2]</sup> However, the limited choice of electrocatalysts that are energy-efficient, selective, and stable increases the complexity of this process.<sup>[3]</sup> Conventionally, metal electrodes have been utilized as electrocatalysts for the aqueous CO<sub>2</sub> reduction reaction, and the product distribution strongly depends on the nature of the electrode surface and the electrolyte.<sup>[3]</sup> Hori and co-workers observed that the CO<sub>2</sub> reduction reaction reproducibly yields CO, CH<sub>4</sub>, HCOOH and other hydrocarbon products and that the selectivity of the products is determined by the nature of the metallic electrode.<sup>[3,4]</sup> Among the various metallic electrodes, copper has attracted

special attentions because it is a metal that produces hydrocarbons during the CO<sub>2</sub> reduction reaction.<sup>[3–13]</sup>

CO is one of the desired products from the reduction of CO<sub>2</sub> with high selectivity because CO can be further reduced to oxygenates and hydrocarbons electrochemically.<sup>[14–16]</sup> Recently, Li and Kanan reported the superior performance of oxide-derived Cu (OD–Cu) in aqueous CO<sub>2</sub> reduction compared to polycrystalline Cu under the identical conditions.<sup>[7]</sup> The OD–Cu electrocatalyst, however, suffers from low product selectivity, co-generating H<sub>2</sub>.<sup>[7,13]</sup> Additionally, although the morphology changes by the oxidation treatment are prominent, the effective active sites on Cu-based surfaces are still under debate, despite a large number of previous studies.<sup>[3–16]</sup> On the other hand, noble metals, including Au and Ag, are electrocatalysts that can efficiently reduce aqueous CO<sub>2</sub> to CO, with selectivities approaching 100%,<sup>[17,18]</sup> but their high cost remains a concern. Non-noble metal bismuth-based electrode necessitates the presence of ionic liquids and non-aqueous phase to demonstrate high performance to generate CO from CO<sub>2</sub>, and the effects of the active components and of the electrolyte remain unclear.<sup>[19]</sup>

Designing a CO<sub>2</sub>-reducing electrocatalyst should thus be focused on the use of non-noble-metals that are selective and energy-efficient. Recently, various strategies have been reported for the conversion of CO<sub>2</sub>, including alloying of copper with other metals,<sup>[20–23]</sup> and for the electrochemical reduction reaction using density functional theory (DFT) calculations to obtain higher selectivity and energy efficiency.<sup>[24–27]</sup> The general trend is that the binding strengths of the intermediates on the catalyst surface need to be adequate and thus the importance of the surface coordinately unsaturated sites has been addressed.<sup>[6,9,11,14,15]</sup> Bimetallic approaches have also been explored by DFT calculations, which may change the conventional electronic structure associated with d-center theory,<sup>[24,25]</sup> and/or geometric and ensemble effects of the metal active sites.<sup>[27]</sup> The competitive interaction of H<sup>+</sup>/water with two metal centers may control the reaction pathway during the electrochemical reduction of CO<sub>2</sub>, promoting the reduction of CO<sub>2</sub> on one or both of the metal centers, thereby resulting in better selectivity. This study focused on an indium electrodeposited Cu electrocatalyst, which resulted in the formation of a Cu–In alloy that works at moderate overpotentials with exclusive selectivity for CO and excellent stability.

OD–Cu substrate was obtained by thermally oxidizing a Cu metal sheet at 773 K for 2 h in static air.<sup>[13]</sup> This treatment led to the formation of a hairy CuO nanowire structure on Cu<sub>2</sub>O–Cu layers,<sup>[13]</sup> resulting in a surface rough-

[\*] Dr. S. Rasul, Dr. A. Jedidi, Dr. Y. Minenkov, Prof. L. Cavallo, Prof. K. Takanabe  
Division of Physical Sciences and Engineering  
KAUST Catalysis Center (KCC)  
King Abdullah University of Science and Technology (KAUST)  
4700 KAUST, 23955-6900 Thuwal (Saudi Arabia)  
E-mail: kazuhiro.takanabe@kaust.edu.sa

Dr. D. H. Anjum  
Advanced Nanofabrication Imaging and Characterization Core Lab  
King Abdullah University of Science and Technology (KAUST)  
4700 KAUST, 23955-6900 Thuwal (Saudi Arabia)

[\*\*] The research reported herein was supported by the King Abdullah University of Science and Technology. L.C. and A.J. are grateful to the KAUST Supercomputing Laboratory for the resources provided under the project k199.

Supporting information for this article (including experimental and theoretical details) is available on the WWW under <http://dx.doi.org/10.1002/anie.201410233>.

ness factor that was increased 140-fold compared to that of the pristine Cu sheet as measured by cyclic voltammetry (Supporting Information, Table S1). The Cu-In electrode was then prepared through electrochemical reduction of the OD-Cu in two-electrode system with a solution containing 0.05 M  $\text{InSO}_4$  and 0.4 M citric acid at a current density of  $-3.3 \text{ mA cm}^{-2}$  for 90 min (ca.  $18 \text{ C cm}^{-2}$ ). This deposition of In underwent a rather complex reduction process in which both reduction of the Cu oxide and deposition of In occurred (Supporting Information, Figure S1). The surface roughness was further improved to double that of OD-Cu (Supporting Information, Table S1).

The as-prepared Cu-In electrode was then tested for the reduction of  $\text{CO}_2$  in a two-compartment, three-electrode electrochemical cell in 0.1 M aqueous  $\text{KHCO}_3$  saturated with  $\text{CO}_2$  ( $\text{KHCO}_3/\text{CO}_2$ ). The results for the reduction of  $\text{CO}_2$  using the OD-Cu and Cu-In electrodes under chronopotentiometric conditions when a geometric current density in the electrode of  $-1.67 \text{ mA cm}^{-2}$  for 1 h are shown in the Supporting Information, Figure S2. An initial transient potential change without the formation of any products was observed, which most likely originates from the reduction of oxide surfaces that are not active for  $\text{CO}_2$  reduction.<sup>[13]</sup> At steady-state electrolysis, the potential was shifted to ca.  $-0.7 \text{ V vs. RHE}$ . Under these conditions, the Cu-In electrode selectively converted  $\text{CO}_2$  to CO with a Faradaic efficiency of about 95 % and with almost negligible levels of  $\text{H}_2$  levels compared to the CO selectivity of 30 % obtained using OD-Cu.

The Cu-In electrode was subsequently tested at different applied potentials and compared with OD-Cu. Figure 1 shows the total current density ( $j_{\text{tot}}$ ) and Faradaic efficiency (FE) at  $-0.3$  to  $-0.7 \text{ V vs. RHE}$  in 0.1 M  $\text{KHCO}_3/\text{CO}_2$ . As shown in Figure 1a, similar values for total current density were obtained for OD-Cu and Cu-In in the same potential range

and electrochemical conditions. These results indicate that the electron transfer rates are essentially identical in these electrodes; however, they exhibited a distinct difference in selectivity. The effects of the applied potentials on the FEs for OD-Cu and Cu-In are shown in Figure 1b and c, respectively. OD-Cu began to convert  $\text{CO}_2$  at a potential of  $-0.3 \text{ V vs. RHE}$ , primarily generating  $\text{H}_2$  as the reaction product. When the electrode was more negatively polarized, the conversion of  $\text{CO}_2$  to CO and  $\text{HCOOH}$  improved, reaching maximum FE of 40 and 30 %, respectively, at  $-0.6 \text{ V vs. RHE}$ , consistent with previous results.<sup>[7,13]</sup> In contrast, the Cu-In electrode catalyzed the reduction of  $\text{CO}_2$  at  $0.3 \text{ V vs. RHE}$ , to CO selectively ( $\text{FE}_{\text{CO}} \approx 23 \%$ ) while suppressing the formation of  $\text{H}_2$  ( $\text{FE}_{\text{H}_2} \approx 3 \%$ ). We were unable to capture the remaining products, probably because of additional Cu and/or In reduction as the  $\text{Cu}/\text{Cu}^{x+}$  or  $\text{In}/\text{In}^{y+}$  standard redox potentials reside in this range.<sup>[28]</sup> Moreover, at applied potentials from  $-0.3$  to  $-0.7 \text{ V vs. RHE}$ , CO was produced as almost the sole product of  $\text{CO}_2$  reduction, approaching an FE of 90 % at  $-0.5 \text{ V vs. RHE}$ . It is clear that the presence of In along with Cu drastically altered the nature of the electroactive species. The partial current density for CO production ( $j_{\text{CO}}$ ) as a function of overpotential (Tafel plot) is plotted in the Supporting Information, Figure S3. The Tafel plot exhibits a slope of greater than  $120 \text{ mV dec}^{-1}$ , similar value to that of OD-Cu,<sup>[7]</sup> which corresponds to a mechanism in which an initial single-electron transfer or adsorption of reactant is the rate-determining step.

To evaluate the stability of the Cu-In catalyst, electrolysis with long controlled potentials in 0.1 M  $\text{KHCO}_3/\text{CO}_2$  at  $-0.6 \text{ V vs. RHE}$  was performed, as shown in Figure 1d. The reaction was intentionally stopped after 3.5 h and allowed to stand overnight to observe the degradation of the electrode under open-circuit aqueous conditions. The reaction was then restarted for an additional 3.5 h. The results indicated that the Cu-In catalyst is extremely stable under the conditions for aqueous  $\text{CO}_2$  reduction, with an 85 % FE for CO for 7 h.

A SEM image of the Cu-In structure is presented in the Supporting Information, Figure S4. The microstructure consists of large irregularly shaped grains ranging from 100 to 500 nm in size. The large grains are formed as a result of the agglomeration of small nanoparticles (ca. 50 nm), which are capped by a shell-like structure. High-resolution transmission electron micrographs (HR-TEM) and the corresponding calculated fast Fourier transform (FFT) patterns of the Cu-In samples after the  $\text{CO}_2$  reduction experiments are shown in Figure 2a. The nanostructure could be divided into two distinct regions: the bulk and the surface. The FFT pattern of the core clearly shows a highly crystalline structure, whereas the FFT pattern of the shell shows a deformed crystal structure, which may arise from the diffusion of In, with a large atomic radius (0.155 nm), into the smaller Cu (0.135 nm) lattice. Superimposed elemental maps of In (green) and Cu (red) are shown in Figure 2b. The Figure clearly shows that the surface is enriched with In with a thickness of about 3 nm. The XRD pattern of the Cu-In sample (Figure 3a) confirms the formation of the Cu-In bimetallic ( $\text{Cu}_{11}\text{In}_9$ ) alloy (PDF 00-065-4963), with intense peaks for the Cu metal substrate (PDF 00-004-0836). The X-

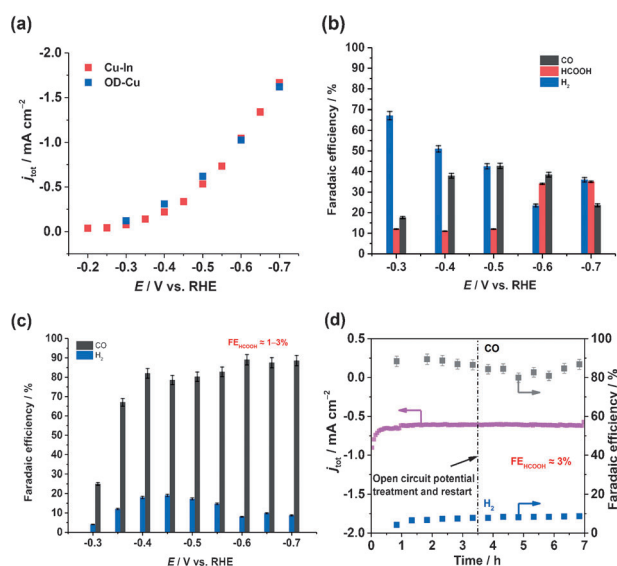


**Figure 1.** a) Comparison of the current density profiles for OD-Cu and Cu-In, chronoamperometric analyses of b) OD-Cu and c) Cu-In, and d) the long-term stability test for the Cu-In catalyst at  $-0.6 \text{ V vs. RHE}$  in 0.1 M  $\text{KHCO}_3/\text{CO}_2$ .

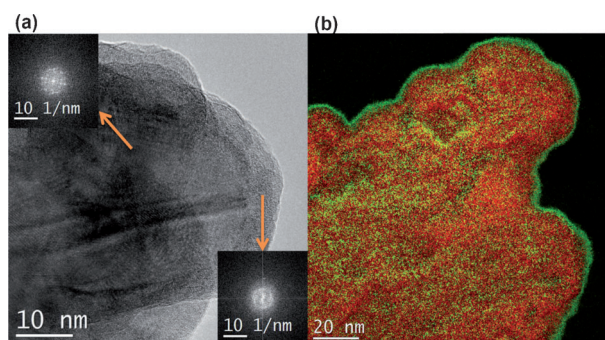


**Figure 2.** a) HR-TEM images of Cu-In with FFT images from the bulk and the surface (inset); b) EDS element mapping of the selected area: In (green), Cu (red).

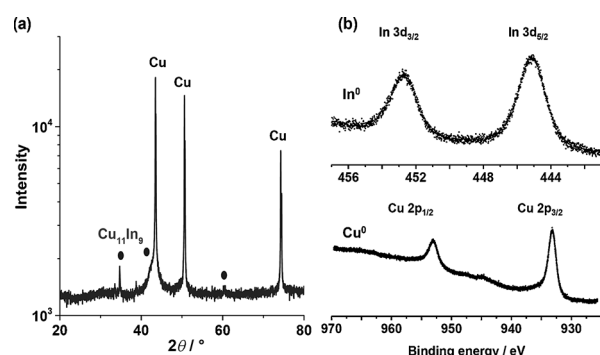


**Figure 3.** a) XRD profiles and b) In 3d and Cu 2p XPS spectra of the Cu-In sample.

ray photoelectron spectra for Cu 2p<sub>3/2</sub> and Cu 2p<sub>1/2</sub> and for In 3d<sub>5/2</sub> and 3d<sub>3/2</sub> (Figure 3b) indicate the reduction to the Cu<sup>0</sup> and In<sup>0</sup> metallic states. Overall, the characterization suggests that the thin layer of bimetallic Cu-In alloy was uniformly formed on the rough surface of OD-Cu.

The experimental data presented here raise a very important question regarding the influence of the environment on the nature of the active species when a second metal center is present along with Cu. A separate CO<sub>2</sub> reduction experiment with an In-deposited Cu sheet without an initial oxidation treatment (Supporting Information, Figure S5) showed only slight improvement in CO selectivity (H<sub>2</sub> predominant), indicating that having OD-Cu as the starting substrate is effective. This result may indicate that the high surface area with grain boundaries,<sup>[7]</sup> and the specific surface facets created by the oxidation/re-reduction treatment are essential for achieving high selectivity toward CO at low overpotentials. Another experiment with an In-deposited In sheet (Supporting Information, Figure S6) resulted in formic acid as the major product with trace amounts of H<sub>2</sub> at elevated overpotentials (typically < −0.9 V vs. RHE), indicating that In alone will not lead to the formation of CO and Cu is essential. Furthermore, a similar increase in selectivity towards CO was observed using Sn and Zn as the second metals (Supporting Information, Figures S7 and S8), suggesting that the universal effects of the second metals that have

high overpotentials toward the evolution of H<sub>2</sub> prevail. When a high hydrogen overpotential metal such as In is present around the Cu active site, effectively forming a Cu-In alloy, it presumably inhibits the formation of H<sub>2</sub> on Cu without deactivating the reduction of CO<sub>2</sub>.

DFT calculations were used to shed light on the effect of In on the bulk and surface properties of pure Cu. Comparison of the DOS of pure Cu and of Cu/In alloys with compositions of up to 50 % In indicated that the presence of In does not significantly affect the electronic structure of pure Cu (Figure 4a; Supporting Information, Figures S10 and S11). Further details of the calculated bulk electronic structure are

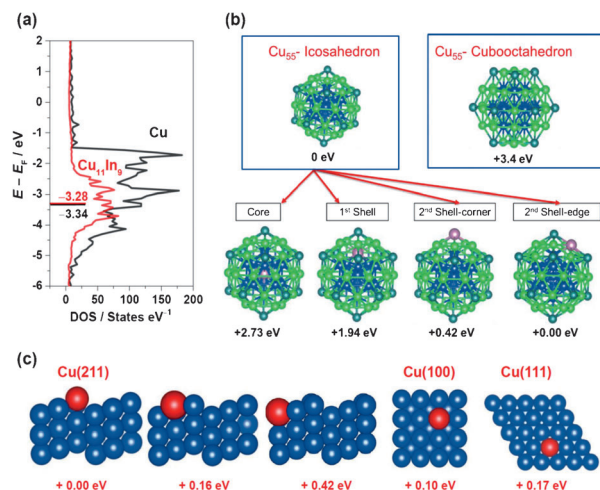


**Figure 4.** a) Density of states of Cu and of Cu<sub>11</sub>In<sub>9</sub>. The values for the d-band center are designated. b) Site preference of In replacing one Cu in Cu<sub>55</sub> (Ih) cluster. The energies relative to Cu<sub>55</sub>-Ih are presented. In the case of Cu<sub>55</sub>-Oh, the same site preference was obtained for In. c) Side views of the three possible geometries of the (211) facet and top views of (100) and (111) facet of Cu with one In atom replacing a Cu atom. The energies relative to the most stable structure (left) is presented.

available in Supporting Information. Consistent with the recent reports,<sup>[27]</sup> this result suggests that the role of In is to locally modify the properties of the surfaces. For this reason, we investigated models of possible geometrical situations occurring at the surface of Cu/In alloys. We thus modeled the effect of replacing one Cu atom by one In atom, as well as the effect of adsorbing an In atom on a perfect Cu surface. Although high In concentrations in the real alloys will result in surfaces that cannot be represented by this model consisting of a single In atom on a pure Cu system, this type of model can offer valuable insights.<sup>[27]</sup>

The first model in the form of the Cu<sub>54</sub>In nanoparticles indicate that the In atom prefers to specifically replace a Cu atom on the edge of the icosahedron, and not by a Cu atom at the corner (Figure 4b). The second model for the relative energy of an In atom replacing one Cu atom on the three facets, (100), (111), and (211), clearly show that the In atom preferentially replaces a Cu atom on top of the step of the



(211) facet (Figure 4c; Supporting Information, Figure S12), followed by replacement of a Cu atom on the (100) facet, +0.10 eV, and by the (111) facet, +0.17 eV. The different stabilities of the different situations, both in the nanoparticle and the surfaces, can be clearly related to the larger size of In compared to Cu. Indeed, the relative stability of Cu replacement on the three considered Cu facets is inversely correlated with the atom density on the surfaces. Moving to In adsorption on a regular Cu facet (Supporting Information, Figure S13), our results clearly indicate that the additional In atom prefers to sit on the groove between steps on the (211) facet, followed by adsorption on the four-fold site of the (100) facet, +0.18 eV, and by adsorption on the three-fold site of the (111) facet, +0.27 eV.

To gather information on the possible impact of a nearby In on the adsorption energy of key intermediates, as an example, we investigated H, CO and COOH adsorption on the (100) facet presenting one In atom (Supporting Information, Figures S14–S18). Our results indicate that the favored H adsorption on the four-fold site is disfavored by 0.12 eV if one of the four Cu atoms is replaced by an In atom, while the CO adsorption energy on top of one of the Cu atoms is substantially unchanged. This suggests that In atoms on the various surfaces of the alloy could reduce the number of multi-fold sites with strong adsorption ability. For COOH\*, the presence of In improves the stability of COOH\* by roughly 0.1 eV, possibly reducing the trend to release HCOOH. Further details for DFT calculation are described in Supporting Information.

The fact that OD-Cu is effective for achieving high CO selectivity suggests that the more electronically unsaturated sites may be associated with the active sites. Our DFT calculation suggests that In, the high-overpotential metal for H<sub>2</sub> formation,<sup>[29]</sup> may cause both local-geometric and local-electronic effects. The In energetically prefers to locate at the edges of the Cu surface (even over the corners). Assuming that In selectively decorates the H<sub>2</sub> evolution sites (for example, presumably edges), the intact Cu corners (kinks) may be still responsible for the selective reduction of CO<sub>2</sub> to CO. The presence of In also causes the weakened adsorption of H over CO. The fact that the In incorporation did not decrease the current density (Figure 1a) suggests that In did not deactivate the catalyst, but most likely enhanced CO<sub>2</sub> or associated adsorbed species, which in turn improves CO<sub>2</sub> reduction selectivity. For this, our results indicate that Cu-In bifunctional sites should be effective as neither Cu nor In alone has this effect. Determining the site requirements for selective CO formation on the Cu<sub>11</sub>In<sub>9</sub> alloy surface requires further detailed studies; however, this investigation presents a potential strategy for developing a selective CO<sub>2</sub> reduction electrode and new insights on possible active sites for the reduction of CO<sub>2</sub>.

In summary, our results show that a Cu-In sample prepared by the in situ reduction of Cu<sub>2</sub>O in an InSO<sub>4</sub> solution selectively catalyzed the reduction of CO<sub>2</sub> to CO with a high FE and with extremely high stability for the electrocatalysis. Moreover, these catalysts suppress the reduction of H<sup>+</sup> and simultaneously promote the conversion of CO<sub>2</sub>, which is highly desired in the electrochemical

recycling of aqueous CO<sub>2</sub>. Additionally, Cu-In electrodes are composed of non-precious metals and can be readily prepared and scaled up for commercial applications. Naturally, this material can also be applied for CO electrochemical conversion.<sup>[16]</sup> Thus, we believe that Cu-In catalyst is the first step toward obtaining efficient, selective and low-cost electrocatalysts in the future.

Received: October 18, 2014

Revised: November 17, 2014

Published online: December 23, 2014

**Keywords:** carbon dioxide fixation · Cu-In alloy · electrocatalysis · electrochemistry · reaction mechanisms

- [1] N. S. Lewis, D. G. Nocera, *Proc. Natl. Acad. Sci. USA* **2006**, *103*, 15729–15735.
- [2] T. A. Faunce, W. Lubitz, A. W. Rutherford, D. MacFarlane, G. F. Moore, P. Yang, D. G. Nocera, T. A. Moore, D. H. Gregory, S. Fukuzumi, K. B. Yoon, F. A. Armstrong, M. R. Wasielewski, S. Styring, *Energy Environ. Sci.* **2013**, *6*, 695–698.
- [3] Y. Hori in *Modern aspects of electrochemistry*, Vol. 42 (Eds.: C. G. Vayenas, R. E. White, M. E. Gamboa-Aldeco), Springer, New York, **2008**, pp. 89–189.
- [4] Y. Hori, H. Wakebe, T. Tsukamoto, O. Koga, *Electrochim. Acta* **1994**, *39*, 1833–1839.
- [5] K. W. Frese, *J. Electrochem. Soc.* **1991**, *138*, 3338–3344.
- [6] Y. Hori, I. Takahashi, O. Koga, N. Hoshi, *J. Phys. Chem. B* **2002**, *106*, 15–17.
- [7] C. W. Li, M. W. Kanan, *J. Am. Chem. Soc.* **2012**, *134*, 7231–7234.
- [8] M. R. Thorson, K. I. Siil, P. J. A. Kenis, *J. Electrochem. Soc.* **2013**, *160*, F69–F74.
- [9] W. Tang, A. A. Peterson, A. S. Varela, Z. P. Jovanov, L. Bech, W. J. Durand, S. Dahl, J. K. Nørskov, I. Chorkendorff, *Phys. Chem. Chem. Phys.* **2012**, *14*, 76–81.
- [10] K. P. Kuhl, E. R. Cave, D. N. Abram, T. F. Jaramillo, *Energy Environ. Sci.* **2012**, *5*, 7050–7059.
- [11] R. Reske, H. Mistry, F. Beharfarid, R. R. Cuenya, P. Strasser, *J. Am. Chem. Soc.* **2014**, *136*, 6978–6986.
- [12] X. Nie, M. R. Esopi, M. J. Janik, A. Asthagiri, *Angew. Chem. Int. Ed.* **2013**, *52*, 2459–2462; *Angew. Chem.* **2013**, *125*, 2519–2522.
- [13] A. T. Garcia-Esparza, K. Limkrailassiri, L. Frederic, S. Rasul, W. Yu, L. Lin, K. Takanabe, *J. Mater. Chem. A* **2014**, *2*, 7389–7401.
- [14] K. J. P. Schouten, Y. Kwon, C. J. M. van der Ham, Z. Qin, M. T. M. Koper, *Chem. Sci.* **2011**, *2*, 1902–1909.
- [15] K. J. P. Schouten, Z. Qin, E. P. Gallent, M. T. M. Koper, *J. Am. Chem. Soc.* **2012**, *134*, 9864–9867.
- [16] C. W. Li, J. Ciston, M. W. Kanan, *Nature* **2014**, *508*, 504–507.
- [17] Y. Chen, C. W. Li, M. W. Kanan, *J. Am. Chem. Soc.* **2012**, *134*, 19969–19972.
- [18] Q. Lu, J. Rosen, Y. Zhou, G. S. Hutchings, Y. C. Kimmel, J. G. Chen, F. Jiao, *Nat. Commun.* **2014**, *5*, 3242.
- [19] J. L. DiMeglio, J. Rosenthal, *J. Am. Chem. Soc.* **2013**, *135*, 8798–8801.
- [20] M. Watanabe, M. Shibata, A. Kato, M. Azuma, T. Sakata, *J. Electrochem. Soc.* **1991**, *138*, 3382–3389.
- [21] W. J. Durand, A. A. Peterson, F. Studt, F. Abild-Pedersen, J. K. Nørskov, *Surf. Sci.* **2011**, *605*, 1354–1359.
- [22] J. Christophe, T. Doneux, C. Buess-Herman, *Electrocatalysis* **2012**, *3*, 139–146.
- [23] D. Kim, J. Resasco, Y. Yu, A. M. Asiri, P. Yang, *Nat. Commun.* **2014**, *5*, 4948.
- [24] A. A. Peterson, J. K. Nørskov, *J. Phys. Chem. Lett.* **2012**, *3*, 251–258.

- [25] H. A. Hansen, J. B. Varley, A. A. Peterson, J. K. Nørskov, *J. Phys. Chem. Lett.* **2013**, *4*, 388–392.
- [26] A. S. Varela, C. Schlaup, Z. P. Jovanov, P. Malacrida, S. Horch, I. E. L. Stephens, I. Chorkendorff, *J. Phys. Chem. C* **2013**, *117*, 20500–20508.
- [27] H.-K. Lim, H. Shin, W. A. Goddard, Y. J. Hwang, B. K. Min, H. Kim, *J. Am. Chem. Soc.* **2014**, *136*, 11355–11361.
- [28] R. Piercy, N. A. Hampson, *J. Appl. Electrochem.* **1975**, *5*, 1–15.
- [29] Z. M. Detweiler, J. L. White, S. L. Bernasek, A. B. Bocarsly, *Langmuir* **2014**, *30*, 7593–7600.
-